Large Deformation Cyclic Tests on Stainless Steel Reinforcing Bars for Reinforced-Concrete Structures in Seismic Regions

Roberto Gori, *University of Padua, Italy*
Enzo Siviero and Salvatore Russo, *Instituto Universitario de Architettura, Italy*

Stainless steel reinforcing bars, proposed for use in reinforced-concrete (r/c) structures, are available with the same lengths and current diameters of conventional carbon steel bars. They present advantages as regards durability, and anti-oxidability, and mechanical properties. These may make them economically competitive with conventional steel bars, and therefore suitable for use in bridge decks in severe environments. Recent earthquakes have further emphasized the need for metal reinforcements capable of resisting considerable and often repeated deformations. The problem is particularly acute in the case of continuous-beam viaducts, since severe strain comes to bear on the integral joints between the deck and the piers. A solution is the use of stainless steel bars because of their intrinsic stress-strain features. R/c seismic-resistant structures may benefit from stainless steel bars as reinforcement for their higher ductility and toughness. These mechanical properties are particularly suitable for critical regions of r/c continuous beams or frames, as the capability of energy dissipation as well as the ductile elongation are greater than for conventional carbon steel. In addition, the antioxidability property of reinforcing bars affects the durability of the structure and its serviceability. Comparative experimental static monotonic and cyclic large deformation uniaxial tests have been carried out until failure on stainless steel AISI 304L bars with different strain rates, in order to reproduce the actual behavior of steel for r/c structures. Cumulative plastic damage has been also analysed. Initial results reveal a significant dependence of fatigue parameters on the strain rate, particularly for relatively small plastic strain ranges.

Stainless steels are ferrochromium or ferrochromium-nickel alloys with a high corrosion resistance, even at high temperatures, because of their high content of chromium (more than 12 percent) and nickel, which promotes the formation of a passive layer with a considerable chemical inertia in certain ambient conditions. According to the microstructure of the matrix, these steels can be grouped into three major categories: martensitic, ferritic, and austenitic stainless steels.

Martensitic stainless steels have a carbon content of 0.10 to 1.10 percent and have excellent mechanical features in terms of tensile strength and a fair corrosion resistance. Heat treatments can be performed on these alloys as on ordinary steels for hardening and tempering.

Ferritic stainless steels are ferrochromium alloys with lower carbon content and a higher percentage of chro-

mium (17 to 26 percent). They are unsuitable for hardening treatment.

The austenitic steels are the most valuable and most studied of the stainless alloys, as they are best suited to resisting humid corrosive phenomena. They are used in a variety of sectors because of their well-demonstrated corrosion resistance and very high ductility, in addition to the high yield strength they can achieve with work hardening. For these properties, this type of steel can be used successfully in the form of ribbed bars for reinforced concrete structures. In civil works, the carbon steel reinforcement in standard and prestressed reinforced concrete is prone to chemical and electrochemical oxidation, with a consequent progressive reduction in the load-bearing capacity of the structure as a whole (*1*). Therefore corrosion-resistant steel has been recommended (*2*) especially for use in conditions in which the risk of pollution from chlorides is high, such as in sections of road where salt is used to prevent freezing, in reinforced concrete structures in seaside areas, or in environments with problems of aggressive smog.

The stainless steel used as reinforcing bars in concrete can be of three types:

1. AISI 304 (or AISI 304L if welded joints are required) for polluted environments,
2. AISI 316 (or AISI 316L if welded joints are required) for environments containing considerable proportions of chlorides; or
3. AISI 329 biphasic for strongly aggressive ambient conditions involving considerable tensile stresses and high working temperatures.

The use of stainless steel reinforcement is all the more advisable in the case of reinforced concrete structural elements in seismic areas, because it combines the advantages of corrosion resistance (*3,4*) with high ductility and tensile strength (*5*) and, above all, it has a greater dissipating capacity in the plastic deformation range when repeated cycles occur (*6,7*).

Stainless steel bars have already been cyclically tested by others; for example, Ciampoli and Mele (*6*) increased the strain range, where the high slenderness of the specimens, for small diameters, characterized the behavior in compression fields, due to buckling of bars. The aim of this work was to test the tenacity and the cyclic behavior to collapse of stainless steel bars (AISI 304L) in large deformation ranges, and to investigate their dependence on the strain rates, especially regarding strength deterioration.

In the present research, the authors used the experience reached in other cyclic tests with large strains (*7–9*). Cyclic axial loads were applied, imposing for each test prescribed symmetric strain excursions in the plastic range (up to 16 percent) with constant strain rates, corresponding to vibration natural frequencies typical of reinforced concrete bridges. Particular attention was devoted to avoiding the buckling of specimens.

In a previous paper by the authors (*10*), resilience tests were performed to evaluate very good localized behavior in the case of impact. In the same paper, monotonic tests were carried out on stainless steel and conventional carbon steel bars. Again, bond characteristics have already been tested. They do not differ substantially from conventional carbon steel bars.

Notation

δ_i = plastic excursion of each cycle i,
$\delta_{u,\text{mon}}$ = monotonic test plastic excursion,
ϵ = deformation of steel,
ϵ_u = uniform elongation,
ϵ_y = deformation at yield,
$\epsilon_{r5\phi}$ = deformation at the collapse on five diameter length,
ϕ = diameter of steel specimen,
μ_i = ductility of each cycle i,
$\mu_{u,\text{mon}}$ = monotonic test ductility,
A, b = cumulative damage structural constants,
D_F = damage functional,
f_t = tensile strength of steel,
f_y = tensile stress at yield of steel,
n = total number of plastic cycles,
N_i = number of symmetric cycles to failure with the same plastic excursions δ_i.

Inelastic Cyclic Behavior of Metals

Several theories describe the inelastic cyclic behavior of metals, among them the isotropic hardening theory of Hill (*11*); the kinematic hardening theory of Prager, modified by Shield and Ziegler (*12,13*); and the theories of Mroz (*14,15*) and those of Peterson-Popov (*16,17*).

For strain-hardening materials, the yield function changes progressively, whereas for an elastic-perfectly-plastic material, it is constant after yield. A hardening rule is needed to describe how the yield function changes. In stress space, a change of the yield function corresponds to a variation of size, shape, and position of the yield surface. The isotropic hardening rule corresponds to an expansion of the yield surface without any change of shape and of the origin in 3D principal stress space. The kinematic hardening rule corresonds to a translation of the yield surface without any change of size or shape. Both rules do not agree exactly with experimental tests. In particular, the isotropic rule is inexact in predicting elastic behavior for constant stress cycles, while the kinematic rule is generally incorrect in

describing stable hysteresis cycles. Thus, for cyclic behavior, a combination of the isotropic and kinematic hardening rules must be employed with the yield surface allowed to expand and to translate.

A number of formulations have been developed. A very general formulation (*16,17*) distinguishes two limiting material states: a virgin state (strength and hardening defined in the first half cycle of loading), and a fully cycled state. The transition from the virgin state to the fully cycled state is controlled by a weighting function based on accumulated strain. A model based on the principles of this theory and extending the Mroz model to cyclic phenomena was developed (*18*) with combined isotropic and kinematic hardening. However, to give an engineering answer to the problem of finding a general definition of plastic collapse under cyclic loadings, it has been proposed to use normalized damage functionals (*19*), varying from 0 (no plastic damage) to 1 (failure).

Some methods use the hysteresis energy as the damage parameter (*20*): collapse occurs when the structure dissipates an energy equal to a limit value. Other methods are based only on the measure of ductility, neglecting cycle history. More advanced methods (*21*) take into account energy and ductility. A method that considers the actual distribution of plastic cycles and generalizes the linear cumulative law of plastic fatigue (*22*) was developed by Cosenza et al. (*19*). In the present paper, an application of this method was carried out for cyclic uniaxial tests on stainless steel bars for different strain rates.

Experimental Procedures

Monotonic and cyclic tests were carried out by using a universal Dartec actuator (1200 kN, working pressure 207 bar) with two hydraulic grips with variable high 150 to 1050 mm. The lateral compression on specimens was 200 bar.

Monotonic tensile tests were performed according to ISO 6892 (1984), using different rates for elastic and plastic phases. Cyclic tests were carried out using strain control with three different constant strain rates of 6500, 13 000, and 26 000 με/sec, which correspond to relative displacement rates of the grips of 0.25, 0.50, and 1.00 mm/sec.

TABLE 1 Chemical Composition (%) of Tested Steel

C	Si	Mn	P	S	Cr	Ni	Mo	Cu
0.034	0.48	1.48	0.032	0.025	18.46	8.56	0.56	0.45

TABLE 2 Mechanical Characteristics of Stainless Steel Specimens

	f_y (MPa)	f_t (MPa)	f_t/f_y	ε_y (%)	ε_u (%)	$\varepsilon_{r5\phi}$ (%)
ϕ 10	723.60	850.32	1.18	1.89	11.26	21.05
ϕ 12	716.20	849.36	1.18	1.68	10.02	21.05

These tests were carried out on specimens with diameters of 10 and 12 mm in the central part obtained from 32-mm-diameter bars of stainless steel (AISI 304L), the chemical composition of which is shown in Table 1. Specimen length was 140 mm, with a base for measures of 38 mm, and 26-mm-diameter threaded heads (in order to allow the reversal of loading) (*7*).

Monotonic Tests

Results of monotonic tensile tests for the two specimens are shown in Table 2. Even if only a small number of tests was carried out, the results present very good characteristics as regards ductility requirements (*23*). In particular, the excellent values of ϵ_u, together with the high values of f_t/f_y, make them respect class S (seismic) of the CEB-FIP code ($\epsilon_u > 6$ percent and $f_t/f_y > 1.15$) (*24*) and class H (high ductility) of the EC2 code ($\epsilon_u > 5$ percent and $f_t/f_y > 1.08$) (*25*). The very high value of $\epsilon_{r5\phi}$ must be stressed, which could make them respect the lower limits (6, 9, 12 percent) of the EC8 code (*26*), even if stress ratio requirements are slightly higher. In stainless steel, the specific deformation energy prior to necking is significantly high, about twice that of the conventional carbon steel FeB44k, which confirms the results of previous tests (*10*).

Cyclic Tests

All cyclic tests were carried out as constant strain cycling by imposing the upper and lower symmetric limits for plastic strain, with constant strain rates, as specified above, of 6500, 13 000, and 26 000 με/sec (relative displacement rates of the grips of 0.25, 0.50, and 1.00 mm/sec). All the tests were performed until collapse of the specimens. Plastic strain ranges considered, for both diameters ϕ10 and ϕ12, were +2.5 to −2.5 percent;

TABLE 3 Number of Cycles to Failure for Symmetric Large Deformation Uniaxial Tests on Stainless Steel Bars, AISI 304L

	plastic range	+2.5%-2.5%	+5%-5%	+7%-7%	+8%-8%
	strain rate (με/s)				
ϕ 10	6500	34	11	5	4
	13000	46	8, 10	5, 8	4
	26000	58	17,9	6	4
ϕ 12	6500	24	13	8	5
	13000	112,64,65	22, 14, 19	9	7
	26000	99,74,90	12, 11, 13	9	7

+5 to −5 percent; +7 to −7 percent; +8 to −8 percent (7). The number of symmetric cycles to failure is shown in Table 3.

The shapes of the stress-strain curves seem to follow with good agreement the isotropic hardening rules.

The total plastic excursions versus the number of cycles to failure were reported in logarithmic scales for the three different strain rates in Figure 1 (for specimens ϕ10) and in Figure 2 (for specimens ϕ12), obtaining bilogarithmic diagrams of plastic fatigue.

As an example of the cyclic strength deterioration, Figures 3 and 4 report the ratios between the stress peaks at reversal (compression stress or tensile stress) versus the number of hysteresis cycles for ϕ10-mm specimens in symmetric cyclic tests with axial plastic strain ranges +2.5 to −2.5 percent (Figure 3) and for ϕ12-mm specimens in symmetric cyclic tests with axial plastic strain ranges +5 to −5 percent (Figure 4) for two strain rates 13 000 and 26 000 με/sec (displacement rates 0.50 and 1.00 mm/sec).

Analysis of Results

From results of the above monotonic and cyclic tests, it has been possible to evaluate for different strain rates, the two parameters that characterize the linear cumulative law of plastic fatigue.

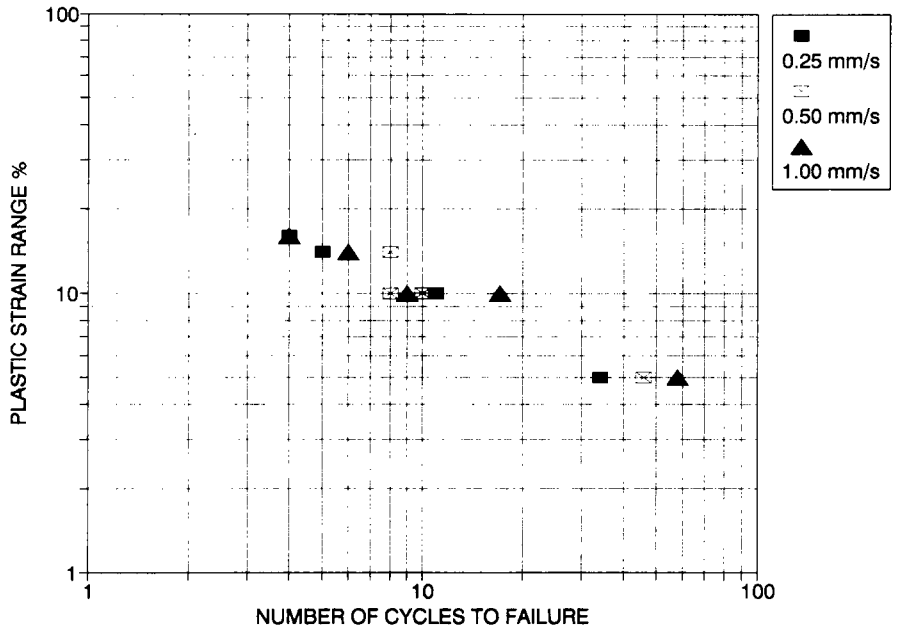

FIGURE 1 Symmetric uniaxial cyclic tests on AISI 304L stainless steel specimens ϕ10 mm in diameter; plastic strain range versus number of cycles to failure for constant strain rates of 6500, 13 000, and 26 000 με/sec (relative displacement rates of the grips of 0.25, 0.50, and 1.00 mm/sec).

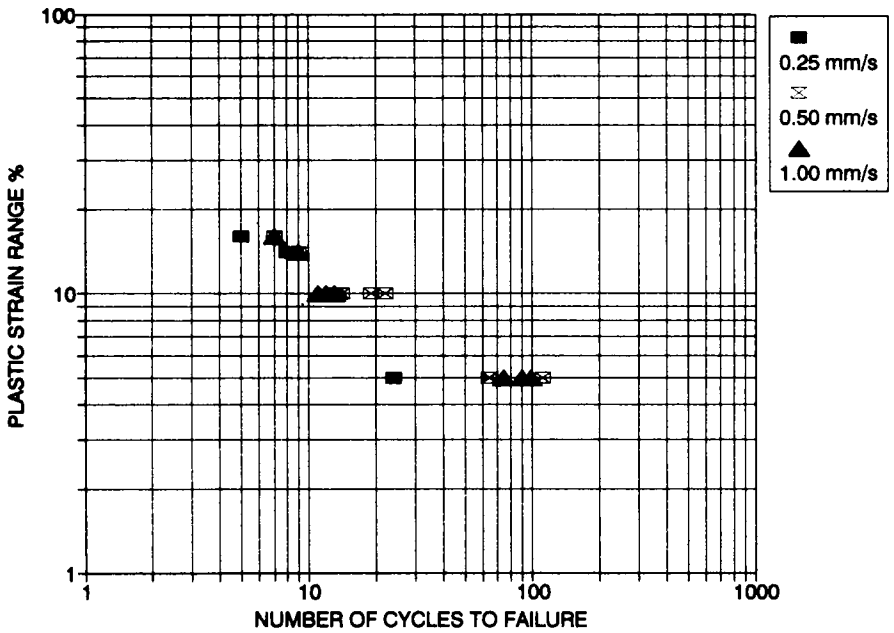

FIGURE 2 Symmetric uniaxial cyclic tests on AISI 304L stainless steel specimens ϕ12 mm in diameter; plastic strain range versus number of cycles to failure for constant strain rates of 6500, 13 000, and 26 000 $\mu\epsilon$/sec (relative displacement rates of the grips of 0.25, 0.50, and 1.00 mm/sec).

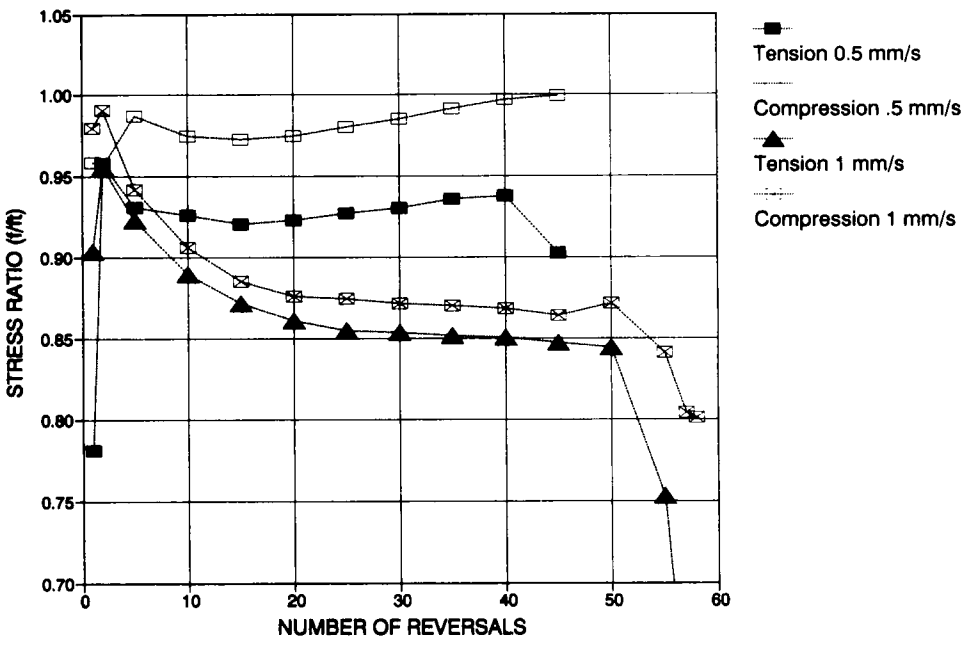

FIGURE 3 Stress ratio for peaks versus number of reversals for two AISI 304L stainless steel specimens, ϕ10 mm in diameter, for symmetric cyclic tests with axial plastic strains between 2.5 and −2.5 percent, for constant strain rates of 13 000 and 26 000 $\mu\epsilon$/sec (relative displacement rates of the grips of 0.50 and 1.00 mm/sec).

The damage functional D_F, which takes into account the different amount of plastic displacement, can be obtained by using the law of cumulative damage (*22,27*), generalizing the Coffin and Mason and Miner laws:

$$D_F = A\sum_{i=1}^{n}(\mu_i - 1)^b \tag{1}$$

where A and b are structural constants to be determined by means of experimental tests, n is the total number of plastic cycles, and μ_i is the ductility (kinematic or cyclic) corresponding to the generic plastic displacement (*19*).

The parameter A can be evaluated by means of a monotonic test carried through to failure (*28*):

$$A = (\mu_{u,\text{mon}} - 1)^{-b} = (\delta_{u,\text{mon}})^{-b} \tag{2}$$

where $\delta_{u,\text{mon}}$ is the corresponding plastic excursion.

Parameter b can be evaluated as the angular coefficient of the line that describes, in logarithmic scales, the equation

$$\log(A) + \log(N_i) + b\log(\delta_i) = 0 \tag{3}$$

which represents the linear damage cumulative law for a test with N_i cycles with the same plastic excursions δ_i, carried through failure (*28*):

$$D_F = A \cdot N_i \cdot (\delta_i)^b = 1 \tag{4}$$

Even if the number of tests was very small for this first campaign, b was evaluated for each strain rate by means of Equation 3 as the mean slope of lines in the two bilogarithmic diagrams of plastic fatigue in Figure 1 (for ϕ10 mm) and in Figure 2 (for ϕ12 mm). Then, using Equation 2 or measuring the y coordinate for $\log(N_i) = 0$ in the bilogarthmic diagrams, the parameter A can be evaluated. It must be noted that the former requires knowledge of the monotonic tests for the different strain rates.

Values of b and A had been already found in a previous paper by the authors (*7*) for a small number of specimens with diameters of ϕ10 mm and ϕ12 mm, respectively, for a constant strain rate of 13 000 $\mu\epsilon$/sec (displacement rate 0.50 mm/sec). These results were substantially confirmed in this second campaign; for tests with that strain rate, average values b = 2.05 to 2.06 and A = 11.41 to 6.28 were found for specimens with diameters of ϕ10 mm and ϕ12 mm, respectively.

Tests with the other strain rates furnished the following results. For a constant strain rate of 6500 $\mu\epsilon$/sec (displacement rate 0.25 mm/sec), average values of b = 1.83 to 1.73 and A = 8.05 to 4.31, and for a constant strain rate of 26 000 $\mu\epsilon$/sec (displacement rate 1.00 mm/sec), average values of b = 2.24 to 2.20 and A = 14.83 to 8.40 were found for specimens with diameters of ϕ10 mm and ϕ12 mm, respectively.

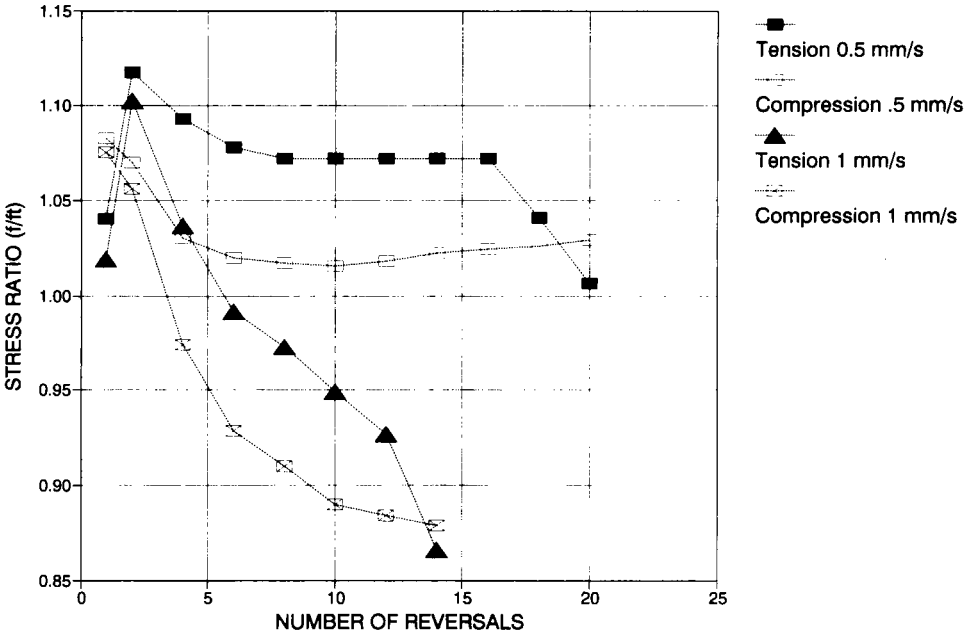

FIGURE 4 Stress ratio for peaks versus number of reversals for two AISI 304L stainless steel specimens, ϕ12 mm in diameter, for symmetric cyclic tests with axial plastic strains between 5 and −5 percent, for constant strain rates of 13 000 and 26 000 $\mu\epsilon$/sec (relative displacement rates of the grips of 0.50 and 1.00 mm/sec).

The different slenderness of the specimens and the nonhomogeneous composition of the core of the original bar are probably responsible for the different behavior of the two specimens.

Conclusions

The bars for reinforced-concrete seismic-resistant bridges can be used in stainless steel alloys with very good results for their high toughness and ductility, as well as for their great capability of energy dissipation and good performances as regards resilience. Furthermore, the well-known antioxidability property of these bars plays a very important role as regards the durability of the structure and the serviceability limit state. At present the site cost of stainless steel bars is about fives times that of high resistant steel. This cost can be reduced in case of large market conditions.

The campaign of experimental monotonic and cyclic tests was carried out on stainless steel bars, and parameters that characterize the linear cumulative law of plastic fatigue were evaluated for uniaxial cyclic tests for different strain rates. Even if only a small number of tests was carried out, the results were good from the mechanical point of view. At this point of the research, the following conclusions can be drawn:

- Stainless steel has a high tensile strength as a result of work hardening;
- The total ductility of stainless steel is considerable and generally very regular;
- Stainless steel specimens present very good characteristics as regards ductility and strength requirements: the excellent values of ϵ_u, together with the high values of f_t/f_y, make them respect class S (seismic) of the CEB-FIP code and class H of the EC2 code;
- This type of lattice, with its larger number of sliding systems, is also responsible for the constantly ductile behavior of stainless steels whatever the conditions of load (even pulsing) and temperature, this feature marking an important difference with respect to conventional carbon steels;
- In stainless steel, the specific deformation energy prior to necking is significantly high (about two that of the conventional carbon steel) which confirms its considerable dissipating features; and
- The strain rate seems to influence the plastic fatigue parameters: constant b increases in a significant way, while constant A decreases, in a minor way, when strain rate increases.

Future steps in the research will deal with the influence of strain rates on cyclic behavior of more ductile stainless steel bars and the comparison with conventional carbon steel bars.

ACKNOWLEDGMENT

The research discussed in this paper was supported by Italian Ministero dell'Università e della Ricerca Scientifica e Tecnologica.

REFERENCES

1. Mele, M., and E. Siviero. Considerazioni generali sulla durabilità delle strutture in c.a. e c.a.p. In *Problemi avanzati per la costruzione di ponti*, CISM, Udine, 1991.
2. Siviero, E. Durability of Reinforced Concrete Structures and Use of Stainless Steel. *Proc., Steel '90*, Genova, May 1990.
3. Flint, G. N., and R. N. Cox. The Resistance of Stainless Steel Partly Embedded in Concrete to Corrosion by Sea Water. *Magazine of Concrete Research*, No. 40, 1988.
4. Kulessa, G. Stainless Steel Reinforcement for Concrete. *Betonwerke + Fertigteil – Technik*, Marz 1988.
5. Paolucci, G. M., E. Siviero, S. Rasera, and G. Barba. Ductility of Stainless Steel Rebars. *CEB Bulletin d'information*, No. 218, 1993.
6. Ciampoli, M., and M. Mele. Comportamento ciclico di barre di acciaio inossidabile per c.a. *Proc. Giornate AICAP '91*. Spoleto, 1991.
7. Gori, R., E. Siviero, and S. Russo. Cyclic Tests on Stainless Steel Reinforcing Bars for r.c. Bridges in Seismic Regions. In *Proc., 2nd International Conference on New Dimensions in Bridge and Flyovers*, Ipoh, Malaysia, October 1994, pp. 75–80.
8. Gori, R., and L. Briseghella. Comportamento ciclico di barre di acciaio ad alta duttilità per calcestruzzo armato in campi di deformazione post-elastici contenuti. *CEB Italia Notizie*, No. 5, Venezia, Maggio 1993.
9. Gori, R. Indagini sperimentali sul comportamento ciclico a compressione di calcestruzzi confinati con spirali di acciaio. *Studi e Ricerche*. No. 14, Scuola di specializzazione in Costruzioni in C.A. e C.A.P., 1993.
10. Paolucci, G. M., R. Gori, E. Siviero, and G. Barba. The Use of Stainless Steel Bars as Reinforcement of R/C Structures in Seismic Regions. In *Proc., 5th U.S. National Conference on Earthquake Engineering*, Chicago, 1994, pp. II 795–805.
11. Hill, R. *The Mathematical Theory of Plasticity*. Oxford University Press, Oxford, England, 1950.
12. Shield, R. T., and H. Ziegler. On Prager's hardening rule. *ZAMP 9a*. 1958, pp. 260–276.
13. Ziegler, H. A Modification of Prager's Hardening Rule. *Quarterly Journal of Applied Mathematics*, Vol. 17, 1959, p. 55.
14. Mroz, Z. An Attempt to Describe the Behaviour of Metals, Under Cyclic Loads Using a More General Workhardening Model. *Acta Mechanica*, Vol. 7, Nos. 2–3, 1969, pp. 199–212.

15. Kujawski, D., and Z. Mroz. A Viscoplastic Material Model and Its Application to Cyclic Loading. *Acta Mechanica*, Vol. 36, 1980, pp. 213–230.
16. Peterson, H., and E. P. Popov. Constitutive Relations for Generalised Loadings. *Journal of the Engineering Mechanics Division*, ASCE, Vol. 103, No. EM4, August 1977, pp. 611–627.
17. Popov, E. P., and H. Peterson. Cyclic Metal Plasticity: Experiments and Theory. *Journal of the Engineering Mechanics Division*, ASCE, Vol. 104, December 1978, pp. 1371–1388.
18. Mosaddad, B., and G. H. Powell. *Computational Models for Cyclic Plasticity, Rate Dependence, and Creep in Finite Element Analysis.* Earthquake Engineering Research Center Report UCB/EERC-82/26, Berkeley, California, 1982.
19. Cosenza, E., G. Manfredi, and R. Ramasco. The Use of Damage Functionals in Earthquake Engineering: A Comparison Between Different Methods. *Earthquake Engineering and Structural Dynamics*, Vol. 22, 1993, pp. 855–868.
20. Briseghella, L., and R. Gori. Indicatori di Danno del Comportamento Sismico di Materiali Soggetti ad Azioni Normali e Taglianti. In *Proc., II Conv. L'ingegneria Sismica in Italia.* Rapallo, Giugno 1984.
21. Park, Y. J., and A. H. S. Ang. Mechanistic Seismic Damage Model for Reinforced Concrete. *Journal of Structural Engineering*, ASCE, Vol. 111, No. 4, April 1985, pp. 722–739.
22. Krawinkler, H., and M. Zohrei. Cumulative Damage in Steel Structures Subjected to Earthquake Ground Motions. *Computers and Structures*, 1983, pp. 531–541.
23. Siviero, E., and S. Russo. Ductility Requirements for Reinforcement Steel. *CEB Bulletin d'information*, No. 218, 1993.
24. CEB-FIP Model Code 1990. *CEB Bulletin d'information No.*, 213/214, T. Telford Ed., 1993.
25. *EUROCODE 2, Design of concrete structures.* Final Draft, 1990.
26. *EUROCODE 8, Strutture in zona sismica. Progetto*, Parte I, 1988.
27. Powell, G. H., and R. Allahabadi. Seismic Damage Prediction by Deterministic Methods: Concepts and Procedures. *Earthquake Engineering and Structural Dynamics*, Vol. 16, 1988, pp. 719–734.
28. Cosenza, E., G. Manfredi, and R. Ramasco. La fatica plastica in ingegneria sismica. *Ingegneria sismica*, Anno X, No. 2, 1993.